JPNT 8(2), 49-58 (2019)
https://doi.org/10.11003/JPNT.2019.8.2.49

JPNT Journal of Positioning, Navigation, and Timing

Gyro Signal Processing-based Stance Phase Detection Method in Foot Mounted PDR

Seong Yun Cho[1†], Chan Gook Park[2]

[1]Department of Robotics Engineering, Kyungil University, Gyeongsan 38428, Korea
[2]Department of Mechanical and Aerospace Engineering, Seoul National University, Seoul 08826, Korea

ABSTRACT

A number of techniques have been studied to estimate the position of pedestrians in indoor space. Among them, the technique of estimating the position using only the sensors attached to the body of the pedestrian without using the infrastructure is regarded as a very important technology for special purpose pedestrians such as the firefighters. In particular, it forms a research field under the name of Pedestrian Dead Reckoning (PDR). In this paper, we focus on a method for step detection which is essential when performing PDR using Inertial Measurement Unit (IMU) mounted on a shoe. Many researches have been done to detect the stance phase where the foot contacts the ground. Most of these methods, however, have a way to detect the specific size of the sensor signal and require thresholds for these methods. This has the difficulty of changing these thresholds if the user is different. To solve this problem, we propose a stance phase detection method that does not require any threshold value. It is expected that this result will make it easier to commercialize the technology because PDR can be implemented without user-dependent parameter setting.

Keywords: PDR, stance phase detection, gyro signal processing, threshold

1. INTRODUCTION

Since the inertial navigation system (INS) has the advantage of calculating the attitude, velocity and position of the moving object even in the environment without the positioning infrastructure despite the large disadvantage of accumulating errors over time, it has become a basic navigation system for the airplane, submarine, and autonomous vehicle (Farrell & Barth 1999). When a person with a low-cost inertial measurement unit (IMU) is a moving object, however, it is obvious that the conventional inertial navigation algorithm alone cannot perform the accurate navigation. To solve this problem, research on pedestrian dead reckoning (PDR) has been conducted for the past two decades. The PDR is based on detecting steps of a pedestrian and estimates strides based on it. Then it combines this information with walking direction to calculate the position of the pedestrian. By using the PDR algorithm instead of the conventional INS algorithm, therefore, it is possible to calculate the position of the pedestrian with small error accumulation over time (Foxlin 2005, Cho & Park 2006, Godha & Lachapelle 2008, Jimenez et al. 2010, Park & Suh 2010, Alvarez et al. 2012, Kang & Han 2015, Tian et al. 2016, Ju & Park 2018).

Research on the PDR using a low-cost IMU has started with mounting an IMU on a shoe (Foxlin 2005, Cho & Park 2006, Godha & Lachapelle 2008, Ju & Park 2018). This is because the part of the human body that is most easily able to detect the step is the foot. Since then, many researches have been done on the detection of steps and stride estimation according to the location of a smartphone for PDR using a smartphone. In the case of holding the smartphone in the hand, in the pocket, on the waist, in the backpack,

Received Feb 18, 2019 **Revised** Mar 29, 2019 **Accepted** Apr 04, 2019
†**Corresponding Author**
E-mail: sycho@kiu.kr
Tel: +82-53-600-5584 Fax: +82-53-600-5599
Seong Yun Cho https://orcid.org/0000-0002-4284-2156
Chan Gook Park https://orcid.org/0000-0002-7403-951X

etc., techniques of recognizing the mounting position and methods of detecting the steps were investigated in each case (Alvarez et al. 2012, Kang & Han 2015, Tian et al. 2016). Here, the accelerometer is mainly used for detecting the step. On the other hand, gyro is sometimes used because it can be difficult to detect a step based on accelerometer at a slow pace (Jayalath et al. 2013). However, it has not been easy to move from a variety of studies to commercialization. In the meantime, the performance of the micro-electro mechanical system (MEMS)-type inertial sensors constituting the low-cost IMU has been improved. Then the IMU's attachment site came back to the shoes. Recently, it has been widely used to drive the PDR with the following algorithm. Based on the INS algorithm, first, the IMU output is used to calculate the attitude, velocity, and position of the foot where the IMU is attached. And detects when the foot contacts the ground. Since the foot velocity is zero at that moment, the zero-velocity update (ZUPT) filter is driven to correct the INS errors. By using the general INS algorithm and the ZUPT filter, it is possible to calculate the position information of the pedestrian with small error accumulation (Jimenez et al. 2010, Park & Suh 2010, Ju & Park 2018). Therefore, detecting the stance phase (SP) when the foot contacts the ground became an important research theme.

Techniques for detecting the steps include peak detection, zero crossing, and flat zone detection. Among these, detecting the SP corresponds to the flat zone detection technique (Cho & Park 2006, Ju & Park 2018). Many researches related to this have been carried out using mainly accelerometer signals. A typical method is to use a bandpass filter. First, the accelerometer output is passed through a high-pass filter: the gravitational acceleration and bias components are removed through the time difference of the accelerometer output. Next, a low-pass filter is derived: the signal corresponding to the high-frequency signal is removed through the moving average of the previously processed signal, and the signal is simplified. Through signal analysis, it can be seen that the signal passed through the low-pass filter has a value close to zero during SP, and this part is detected (Cho & Park 2006). To detect near zero signals over a period of time, a specific threshold is used generally. Two problems arise here. First, there may be a section where the signal is close to zero even while the foot is moving. Second, since the walking characteristics are different for each person, the threshold value in the algorithm should be set differently for each person. So, multiple thresholds must be used in one algorithm, and different thresholds must be set for each person.

In this paper, we propose a SP detection method that does not use a threshold to solve this problem. In this method, gyro signals are used instead of accelerometer signals, and only a low-pass filter using sliding window meaning (SWM) is used instead of the bandpass filter. The positive/negative peaks of the signal simplified by the SWM are detected, and the SP is detected based on it. No threshold is used in this process. This makes it possible for multiple users to use an algorithm without changing parameters. This algorithm is explained in Section 2 of this paper, and the performance of the algorithm is experimentally verified in Section 3.

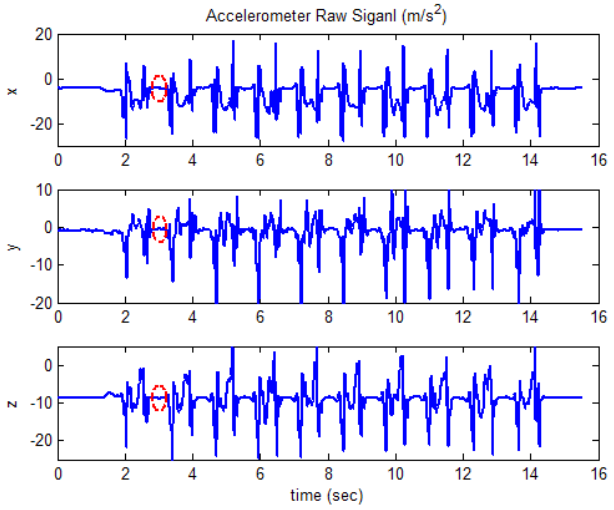

Fig. 1. 3-axis accelerometer raw signals and first stance phase part.

2. A STANCE PHASE DETECTION TECHNIQUE

The IMU, mounted on the shoe, provides gait characteristic signals along the walk through the accelerometer and gyro output. It is important to convert these signals to appropriate signals for SP detection through specific processing. In general, many techniques for detecting SP using the accelerometer signals have been investigated. However, most of these techniques require specific threshold settings. In this Section, signal processing for SP detection is performed using the accelerometer and gyro signals, respectively, and finally the most suitable signal processing technique or SP detection is proposed.

2.1 Accelerometer Signal Processing-based Approach

Fig. 1 shows the output of a 3-axis accelerometer when an IMU with an output frequency of 100 Hz is mounted on the right shoe and a pedestrian walks 10 steps at normal speed. In this figure, the following two facts can be seen: First, the accelerometer output contains the gravitational acceleration

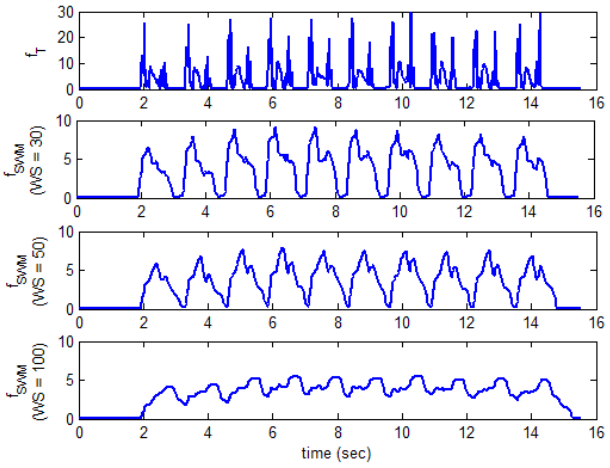

Fig. 2. f_T and SWM values of accelerometer signal according to WS value when walking at normal speed.

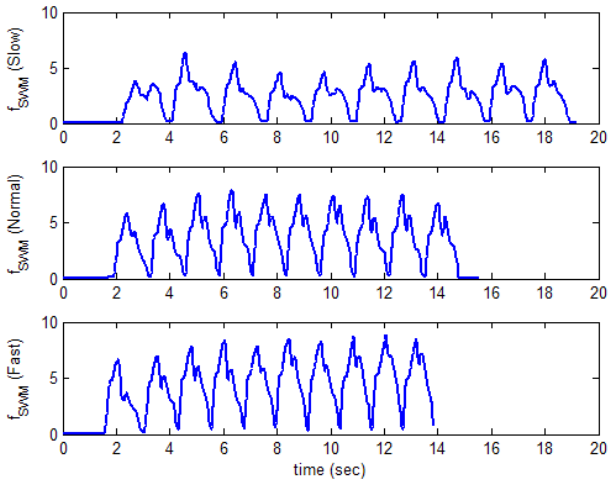

Fig. 3. SWM values of accelerometer signal according to walking speed when WS is set to 50.

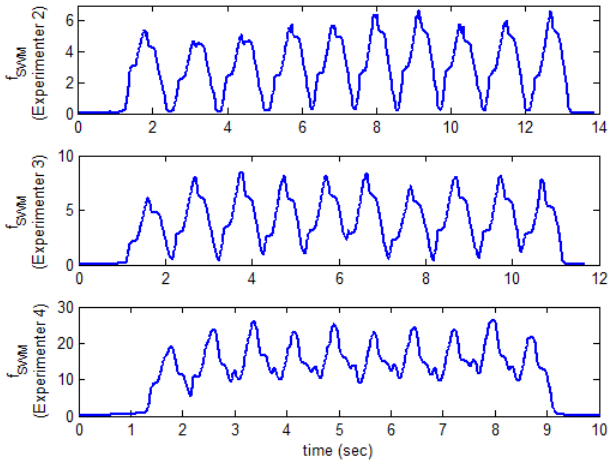

Fig. 4. SWM values of accelerometer signal according to the experimenter when WS is set to 50.

component. Since the IMU is mounted so that the x-axis of the accelerometer is in the forward direction, the y-axis is in the right direction, and the z-axis is in the downward direction of the shoe, it can be seen that the gravitational acceleration is largely reflected on the z-axis output and is larger than the other two axis outputs. The reason why the x- and y-axis accelerometer outputs are not zero during the first 1 second of the Fig. 1 when the foot is stop state is that the attitude of the IMU on the foot is not leveled. Second, a walking pattern appears at each step, and a flat signal appears during the SP. In the figure, the circle represents the first SP. Considering these characteristics, signal processing is performed as shown in Fig. 2 to find the SP.

The first figure in Fig. 2 shows the result of processing the 3-axis accelerometer signals using the following equation.

$$f_{T,k} = \left| \sqrt{f_k^T f_k} - \overline{f}_0 \right| \tag{1}$$

where $f_k = [a_{x,k} \quad a_{y,k} \quad a_{z,k}]^T$ is the 3-axis accelerometer output vector at time k and $\overline{f}_0 = \frac{1}{N}\sum_{i=1}^{N}\sqrt{f_i^T f_i}$ is the value calculated for a certain time (for example, 1 second) in the stop state before the start of navigation to remove the gravitational acceleration component.

f_{SWM} in the Fig. 2 shows the SWM of f_T. Here, the window size (WS) for SWM is set to 30, 50, and 100, respectively. The SWM is used to pass a signal through a low-pass filter to remove the high-frequency component of the signal and to simplify the signal. In this figure, we can see that the WS becomes larger, the signal gets simpler, but the portion corresponding to the SP section becomes smaller. These characteristics vary according to walking-type and speed. In this paper, after various attempts, we set WS to 50, which is half of IMU frequency. The once determined WS is used fixedly with no change according to the walking speed, walking type, and pedestrian. Therefore, the WS determined by the experimental method is different from the threshold for avoiding use in this paper. Compared with f_T, f_{SWM} has a good shape to detect SP. That is, it is only necessary to detect the negative peaks. However, this signal has a different shape depending on the walking speed and the experimenter as shown in Figs. 3 and 4. Fig. 3 shows SWM signals with different walking speed of the same experimenter, and Fig. 4 shows SWM signals according to the experimenter. Fig. 3 shows a relatively good signal form. However, it may be shown in Fig. 4 that signals that are difficult to detect the SP appear depending on the experimenter. Therefore, if the threshold value for detecting the interval corresponding to the SP is set to a small value, the SP may be missed. On the contrary, if the threshold value is set to a large value, multiple

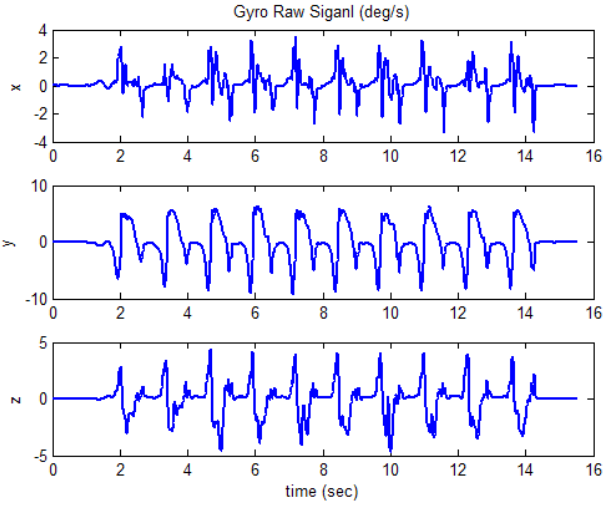

Fig. 5. 3-axis gyro raw signals.

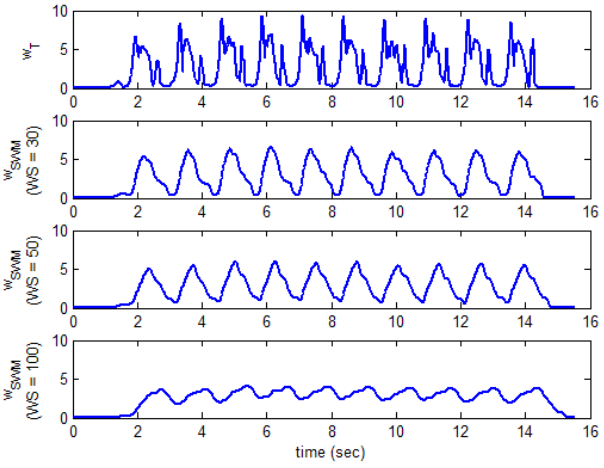

Fig. 6. w_T and SWM values of gyro signal according to WS value when walking at normal speed.

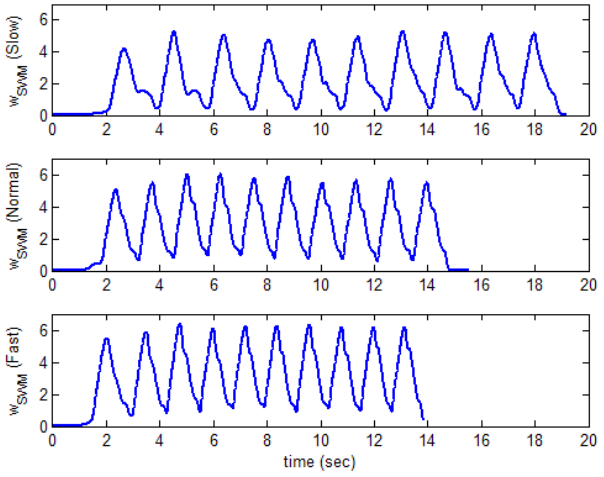

Fig. 7. SWM values of gyro signal according to walking speed when WS is set to 50.

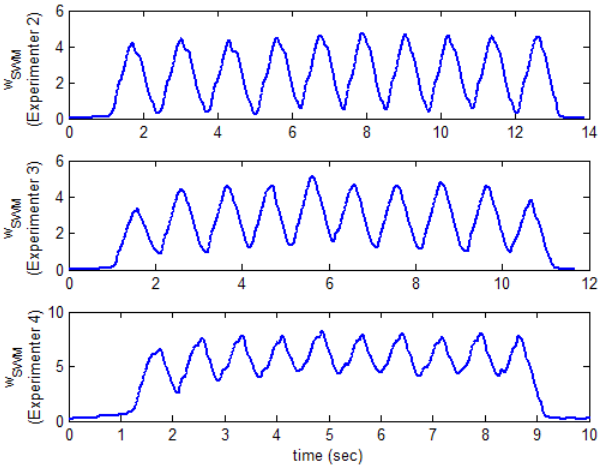

Fig. 8. SWM values of gyro signal according to the experimenter when WS is set to 50.

SPs can be detected during one step. Although the method of adaptively setting the threshold value according to the walking speed may be considered, there arises a problem that different threshold values must be set depending on the pedestrians.

2.2 Gyro Signal Processing-based Approach

Figs. 5-8 show the gyro output and gyro signal processing results matched to Figs. 1-4. w_T is calculated as follows.

$$w_{T,k} = \left| \sqrt{w_k^T w_k} - \overline{w}_0 \right| \tag{2}$$

where $w_k = [g_{x,k} \quad g_{y,k} \quad g_{z,k}]^T$ is the 3-axis gyro output vector at time k and $\overline{w}_0 = \frac{1}{N}\sum_{i=1}^{N} \sqrt{w_i^T w_i}$ is for removing the part corresponding to the gyro bias in the first stop state.

We can see that the negative peak part for SP detection is clear in the figure of SWM which is processed while setting the WS to 50 and changing the walking speed and the experimenter. However, the threshold value for detecting the negative peaks is not easy to set. Fig. 8 shows that the threshold value must be set large for the experimenter 4 to detect the SP. However, if this threshold value is used for the experimenter 3, the SP may not be detected. Even when the signal processing is performed using the gyro output, therefore, it can be confirmed that it is not easy to detect the SP accurately by using the threshold. However, it can be seen that the SWM signal through the gyro signal processing is simpler than the SWM signal through the accelerometer signal processing and is similar to the triangle wave. In this paper, we propose a method to detect the SP using this signal as follows.

The SP can be detected through negative peak detection (NPD), but the positive peak detection (PPD) is performed

first. Figs. 7 and 8 show that the gyro's SWM signal is similar to the incomplete triangle wave. To increase the SP detection accuracy, therefore, the PPD is performed twice and the NPD is performed therebetween. For the PPD, the SWM signal of the gyro is inspected with the interval of size 50 as follows.

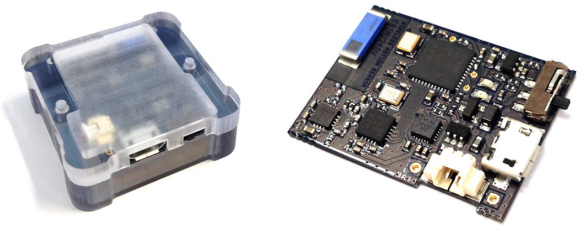

(a) (b)

Fig. 9. IMU used for experiments. (a) outer case (b) internal board

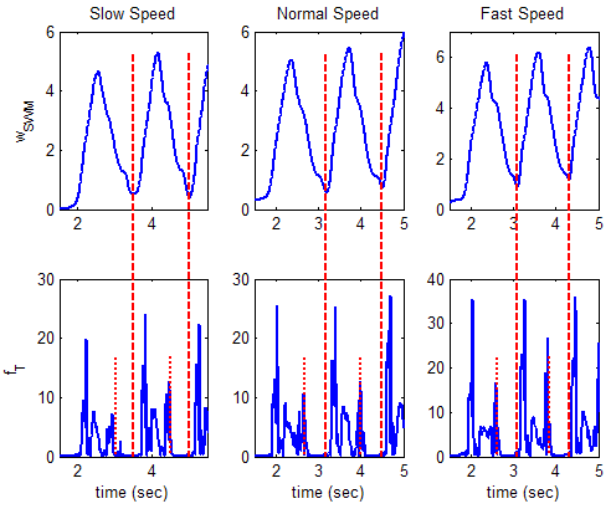

Fig. 10. w_{SWM} and f_T according to walking speed, the time points of the NPD and the points before WS from them.

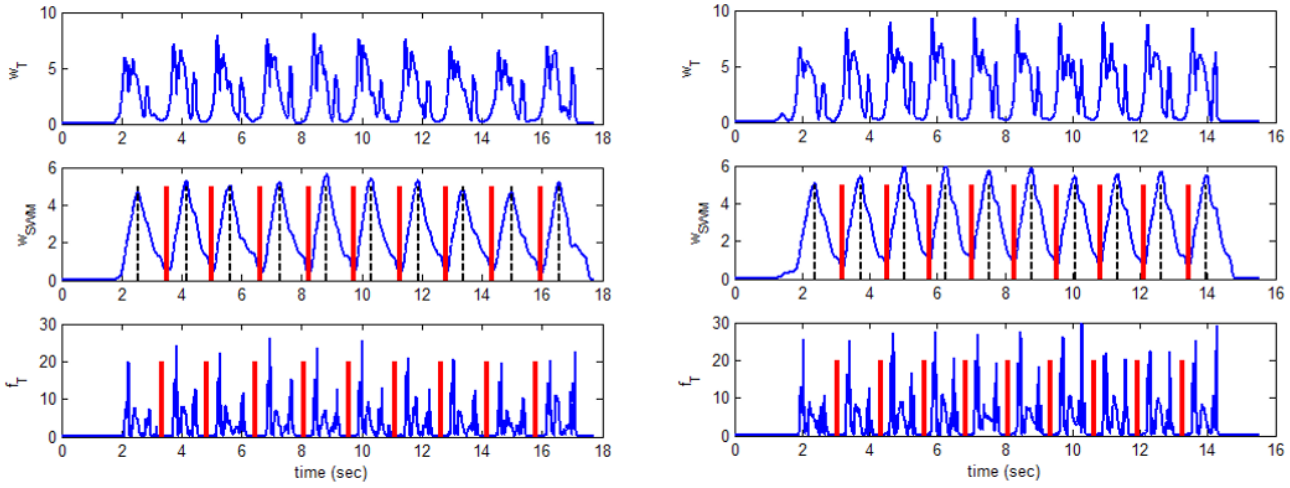

(a) (b)

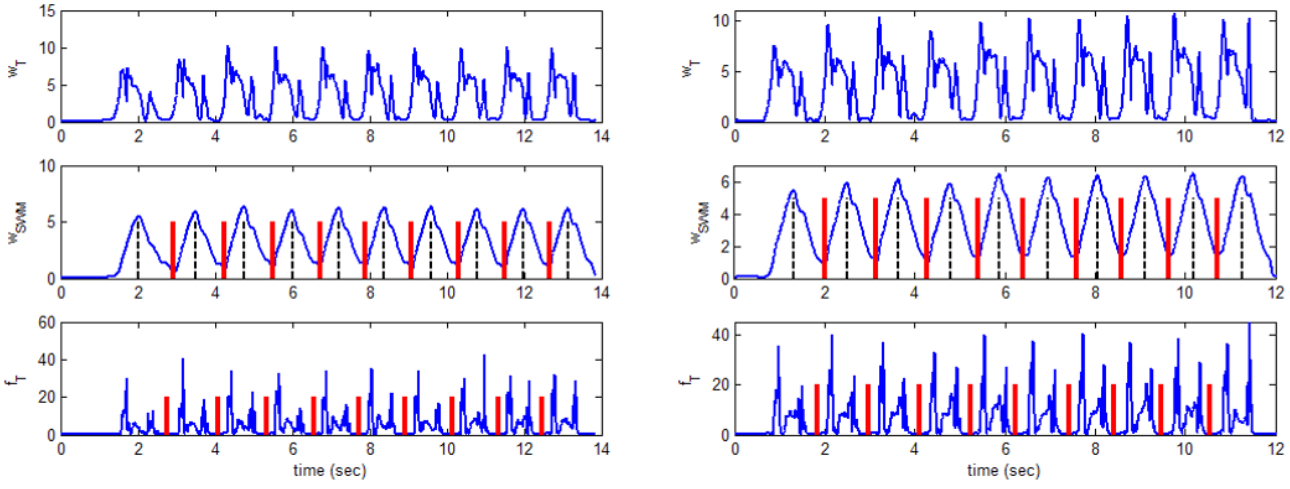

(c) (d)

Fig. 11. SP detection result according to walking speed. (a) slow pace (b) normal pace (c) fast pace (d) very fast pace

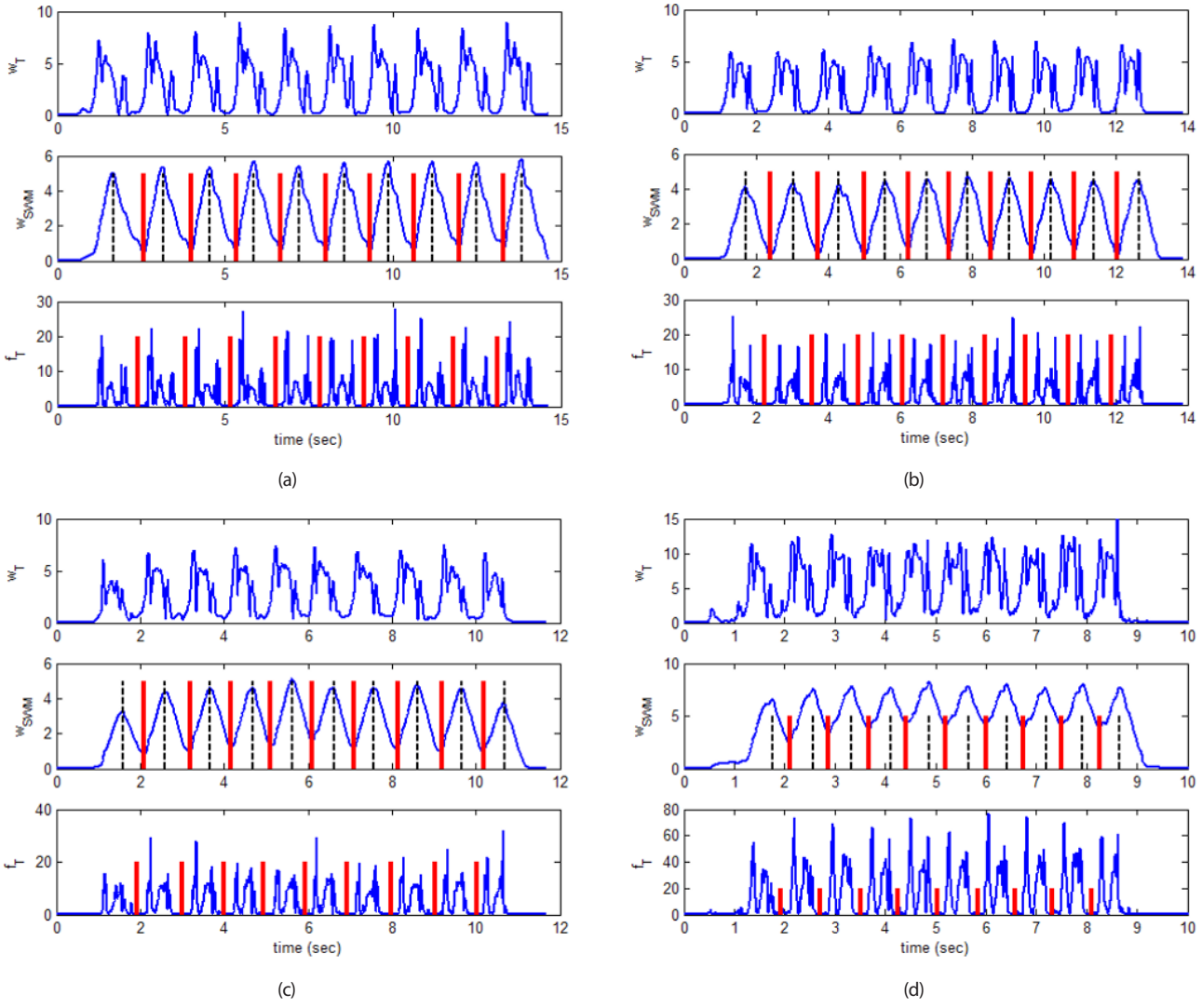

Fig. 12. SP detection result according to the experimenters when walking at normal speed. (a) experimenter 1 (b) experimenter 2 (c) experimenter 3 (d) experimenter 4

If $w_{SWM,k} \geq w_{SWM,k\text{-}1}$
  $cPn = cPn+1$
  $cMn = 0$
Else
  $cMn = cMn+1$
  If $cMn = 0$
    If $cPn > 10$
      Positive peak is detected
    Endif
    $cPn = 0$
  Endif
Endif

If the two PPDs are completed, the part having the smallest SWM signal between the two detection times is detected as the negative peak. The detected negative peak may be present within the SP or may be slightly behind of the SP due to the time delay occurring in the SWM process. In this paper, therefore, it is empirically determined that the SP is the time before WS/3 from the point of detection of the negative peak.

3. EXPERIMENTAL RESULTS

Experiments were performed to verify the performance of the SP detection algorithm proposed in this paper. The IMU used in the experiments is the EBIMU24GV3 manufactured by E2BOX shown in Fig. 9 and has a built-in low-cost accelerometers and gyros for motion detection. This IMU was attached on the right shoe.

The SP detection algorithm was applied according to walking speed, experiment, and walking type, and the results

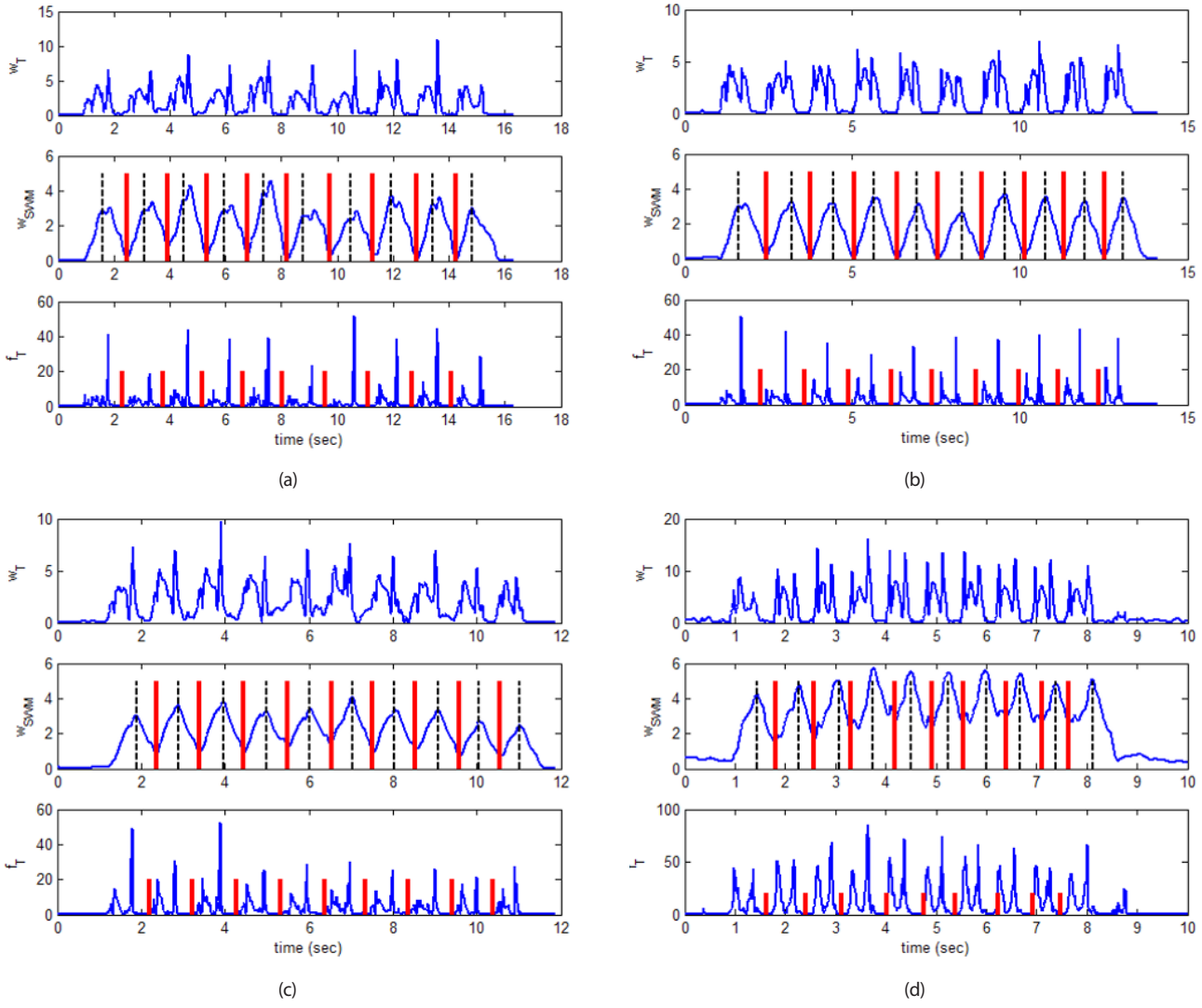

Fig. 13. SP detection result according to the experimenters in backward walking. (a) experimenter 1 (b) experimenter 2 (c) experimenter 3 (d) experimenter 4

are shown in Figs. 10-14.

First, Fig. 10 shows an example of w_{SWM}, and f_T for each walking speed and explains why SP was determined before WS/3 when negative peak is detected. In this figure, the red vertical dashed-lines represent the points of time when the negative peaks are detected, and the red vertical dotted-lines represent the points before WS from the points of the negative peaks. From this figure, it can be seen that there is certainly a SP with a flat value of f_T before the WS/3 from the point when a negative peak is detected regardless of the walking speed.

Fig. 11 shows the SP detection result according to walking speed of the experimenter 1. The experimenter walked 10 steps each at a slow speed, a normal speed, a fast speed, and a very fast speed, and the proposed SP detection algorithm was applied in each case. The first sub-figure of each figure shows

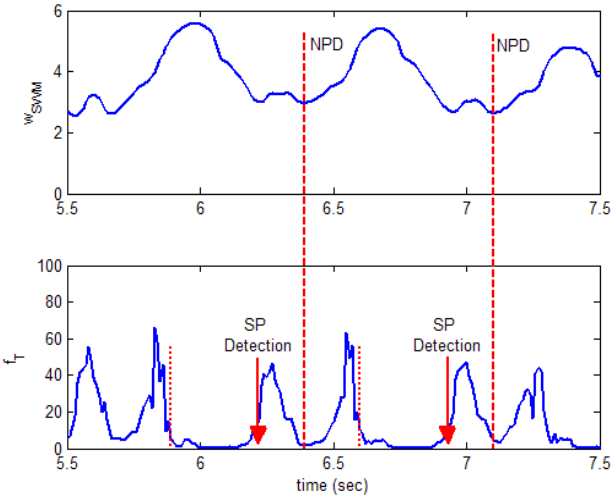

Fig. 14. The zoom-in of Fig. 13d.

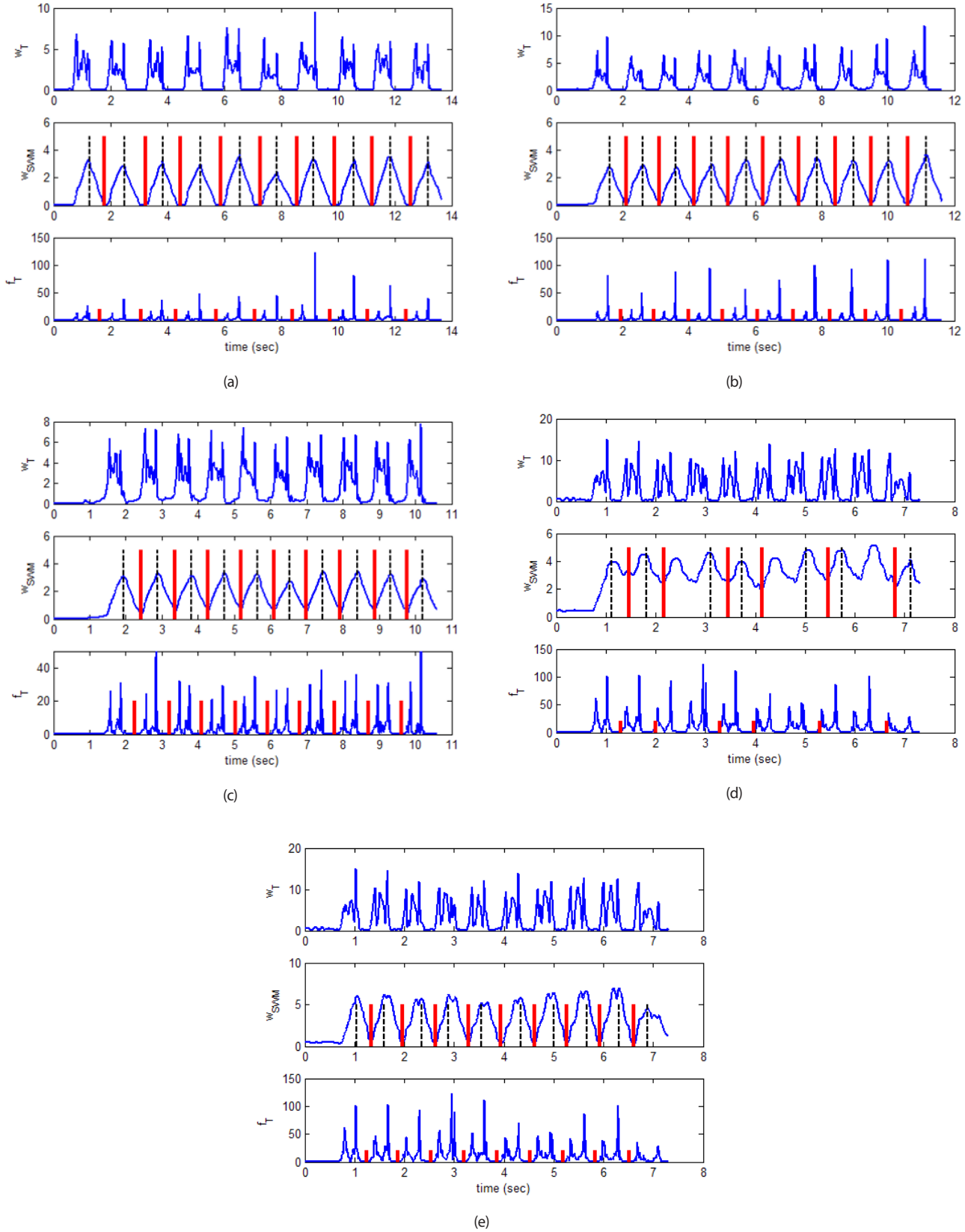

Fig. 15. SP detection result according to the experimenters in left-side walking. (a) experimenter 1 (b) experimenter 2 (c) experimenter 3 (d) experimenter 4 (e) experimenter 4 when setting WS to 25

w_T, and the second sub-figure shows w_{SWM}. In the second sub-figure, the result of PPD using w_{SWM} is shown by vertical dotted-lines and the result of NPD is shown by vertical solid-lines. Regardless of the walking speed, PPD and NPD can be seen to be performed accurately. The third sub-figure of each figure shows f_T and the SP detection positions indicated by red vertical lines. The SPs are detected considering the time delay of the SWM process as explained previously. The point at which the SP is detected is that the foot touches the ground and the f_T value is within a flat zone near zero. From this experimental results, it is confirmed that the SP detection can be accurately performed even if the walking speed is changed.

Fig. 12 shows the result of the SP detection when four experimenters walked at normal speed. The information shown in each sub-figures is the same as Fig. 11. Depending on the walking characteristics of the experimenters, slightly different signal patterns can be seen. However, regardless of the walking characteristics, the f_T becomes a flat signal close to zero while the foot touches the ground. And we can see that SPs are accurately detected within these flat intervals. Therefore, it can be confirmed that the SP detection algorithm proposed in this paper can be considered to produce a good result even when there are different walking characteristics according to the experimenters.

Fig. 13 shows the result of the SP detection when the experimenters perform backward walking. w_T in the case of the backward walking shows a slightly complicated tendency than that in the case of the forward walking. For this reason, when analyzing the w_{SWM} signal, it can be seen that the positive peaks of the experimenter 1and the negative peaks of the experimenter 4 are unclear. Nevertheless, the peak detection algorithm proposed in this paper (detection of positive peaks and then detection of negative peaks between the detected positive peaks) accurately detects positive and negative peaks. Based on this, SPs are detected. In experimenter 3 and 4, however, it can be seen that some SPs were detected at the end of the flat zone of f_T. To analyze this reason, Fig. 13d is enlarged and shown in Fig. 14. Comparing this figure with Fig. 10, it can be seen that when walking backward, the NPD position is much off the flat zone of the f_T. Therefore, the position of WS/3 before NPD is slightly deviated from the stance phase. The detection position adjustment of SP according to the walking type is left as a future study.

Finally, Fig. 15 shows the result of the SP detection when the experimenters make the left-side walk. In this case, w_T shows different characteristics from those of forward and backward walking, and it can be seen that SP detection is clearly performed for the rest of the experimenters except experimenter 4. The w_T of experimenter 4 has a more complex shape than those of other experimenters, and the calculated w_{SWM} is different from the shape sought in this paper. As a result, there is a problem that several positive peaks cannot be detected, and the non-detection of the corresponding SPs also occurs. Experimentally, WS was set to 25 and data of experimenter 4 was re-processed and the result is shown in Fig. 15e. In this case, PPD performance was improved and SP detection performance is also improved. However, changing the WS according to the situation is out of the scope of this paper. Therefore, additional studies to improve the PPD algorithm in the abnormal w_{SWM} signal will be performed later.

From the results of these experiments, it can be seen that the presented SP detection algorithm which does not include the threshold shows excellent results regardless of the walking speed and the experimenters in the forward walking. However, it is necessary to compensate for the time delay of the position of the detected SP in the case of backward and side walking. In addition, in the side walking, there is a research task to improve the PPD algorithm according to pedestrian. Based on the results of this study, we plan to research robust SP detection algorithm regardless of walking speed, walking type, and pedestrian. This algorithm, of course, does not have any threshold.

4. CONCLUSIONS

In this paper, a method for detecting SP in PDR using IMU mounted on a shoe was proposed. The conventional SP detection methods generally use a method of detecting the flat zone through the signal processing of the accelerometer, and different threshold values were used according to the pedestrian. In order to solve this problem, we proposed a technique to detect positive and negative peaks after gyro signal processing and detect SP without threshold. Experiments were carried out with changing the walking speed, the walking type, and the experimenter. The results showed that the proposed method has excellent performance. Future research will be carried out on algorithm for robust SP detection according to walking speed and walking type.

ACKNOWLEDGEMENT

This work was supported by Institute for Information & Communications Technology Promotion (IITP) grant funded by the Korea government (MSIT) (No. 2018-0-00781, Development of human enhancement fire helmet and fire

suppression support system).

AUTHOR CONTRIBUTIONS

Seong Yun Cho contributed to the conceptualization of the idea, implemented the algorithm and wrote the original draft of the manuscript. Chan Gook Park supervised the research and reviewed the manuscript as a project administrator. All authors discussed the proposed approach and results.

CONFLICTS OF INTEREST

The authors declare no conflict of interest.

REFERENCES

Alvarez, J. C., Alvarez, D., Lopez, A., & Gonzalez, R. C. 2012, Pedestrian Navigation based on a Waist-Worn Inertial Sensor, Sensors, 12, 10536-10549. https://doi.org/10.3390/S120810536

Cho, S. Y. & Park, C. G. 2006, MEMS Based Pedestrian Navigation System, Journal of Navigation, 59, 135-153. https://doi.org/10.1017/S0373463305003486

Farrell, J. A. & Barth, M. 1999, The Global Positioning System & Inertial Navigation (NY: McGraw-Hill).

Foxlin, E. 2005, Pedestrian Tracking with Shoe-Mounted Inertial Sensors, IEEE Computer Graphics and Applications, 25, 38-46. https://doi.org/10.1109/MCG.2005.140

Godha, S. & Lachapelle, G. 2008, Foot Mounted Inertial System for Pedestrian Navigation, Measurement Science and Technology, 19, #075202. https://doi.org/10.1088/0957-0233/19/7/075202

Jayalath, S., Abhayasinghe, N., & Murray, I. 2013, A Gyroscope Based Accurate Pedometer Algorithm, International Conference on Indoor Positioning and Indoor Navigation, Montbeliard, France, 28-31 October 2013.

Jimenez, A. R., Seco, F., Prieto, J. C., & Guevara, J. 2010, Indoor Pedestrian Navigation using an INS/EKF Framework for Yaw Drift Reduction and a Foot-Mounted IMU, 7th Workshop on Positioning, Navigation and Communication, Dresden, Germany, 11-12 March 2010. https://doi.org/10.1109/WPNC.2010.5649300

Ju, H. J. & Park, C. G. 2018, A Pedestrian Dead Reckoning System using a Foot Kinematic Constraint and Shoe Modeling for Various Motions, Sensors and Actuators A: Physical, 284, 135-144. https://doi.org/10.1016/j.sna.2018.09.043

Kang, W. & Han, Y. 2015, SmartPDR: Smartphone-Based Pedestrian Dead Reckoning for Indoor Localization, IEEE Sensors Journal, 15, 2906-2916. https://doi.org/10.1109/JSEN.2014.2382568

Park, S. K. & Suh, Y. S. 2010, A Zero Velocity Detection Algorithm Using Inertial Sensors for Pedestrian Navigation Systems, Sensors, 10, 9163-9178. https://doi.org/10.3390/s101009163

Tian, Q., Salcic, Z., Wang, K. I., & Pan, Y. 2016, A Multi-Mode Dead Reckoning System for Pedestrian Tracking Using Smartphones, IEEE Sensors Journal, 16, 2079-2093. https://doi.org/10.1109/JSEN.2015.2510364

Seong Yun Cho received the B.S., M.S., and Ph.D. degrees in Control and Instrumentation Engineering from Kwangwoon University in 1998, 2000, and 2004, respectively. From 2004 to 2013, he was with Electronics and Telecommunications Research Institute as a senior researcher. In 2013, he joined the faculty of the Department of Robotics Engineering at Kyungil University, where he is currently an associate professor. His current research topics include positioning and navigation systems, filtering theory for linear/nonlinear systems, sensors-based motion detection, and LBS application systems.

Chan Gook Park received B.S., M.S., and Ph.D. degrees in Control and Instrumentation Engineering from Seoul National University in 1985, 1987, and 1993, respectively. From 1994 to 2003, he was with Kwangwoon University as an associate professor. In 2003, he joined the faculty of the School of Mechanical and Aerospace Engineering at Seoul National University, where he is currently a professor. His current research topics include advanced filtering techniques, inertial navigation system, GPS/INS integration, MEMS-based pedestrian dead reckoning, and FDIR techniques for satellite systems.